DISCRETE AND CONTINUOUS
DYNAMICAL SYSTEMS SERIES B
Volume **19**, Number **1**, January **2014**

doi:10.3934/dcdsb.2014.19.27

pp. **27–53**

SPECTRAL MINIMAL PARTITIONS OF A SECTOR

Virginie Bonnaillie-Noël

IRMAR, ENS Rennes, Univ. Rennes 1, CNRS, UEB
av. Robert Schuman, F-35170 Bruz, France

Corentin Léna

Laboratoire de Mathématiques d'Orsay, Université Paris-Sud, Bât. 425
F-91405 Orsay Cedex , France

(Communicated by Peter E. Kloeden)

Abstract. In this article, we are interested in determining spectral minimal k-partitions for angular sectors. We first deal with the nodal cases for which we can determine explicitly the minimal partitions. Then, in the case where the minimal partitions are not nodal domains of eigenfunctions of the Dirichlet Laplacian, we analyze the possible topologies of these minimal partitions. We first exhibit symmetric minimal partitions by using a mixed Dirichlet-Neumann Laplacian and then use a double covering approach to catch non symmetric candidates. In this way, we improve the known estimates of the energy associated with the minimal partitions.

1. **Introduction.** In this article, we are interested in the properties of the 'minimal' k-partitions of an open set Ω by k disjoint open sets D_i $(i = 1, \dots, k)$ in Ω. These partitions are minimal in the sense that they minimize the maximum over $i = 1, \dots, k$ of the lowest eigenvalue of the Dirichlet realization of the Laplacian in D_i. Similar problems naturally appear in Biomathematics, to characterize the final states of competition-diffusion systems (e.g. in [11]). In the case of 2-partitions, it is well known that the partition by the nodal domains of a second eigenfunction gives a minimal 2-partition. For $k \geq 3$, although general properties of these minimal partitions have been proved in [7, 9, 8, 17], the minimal k-partitions are generally not known, even for simple domains (see however [17, 4, 18, 15] for some particular examples). The aim of this paper is to exhibit, in the case of angular sectors, some candidates to be minimal k-partitions and to estimate the minimal energy by establishing more accurate bounds than the previously existing ones.

1.1. **Notations and known results.** Let us first state the definition of a minimal partition and review briefly known results about this object that will be useful in our study. In the following, Ω is an open, bounded, and connected set in $\mathbb{R}^2$. We assume that $\partial\Omega$ satisfies some regularity properties. Following [17], we can for

2010 *Mathematics Subject Classification.* Primary: 35B05, 35J05, 49M25, 65F15, 65N25; Secondary: 65N30.

Key words and phrases. Spectral theory, minimal partitions, nodal domains, Aharonov-Bohm Hamiltonian, numerical simulations, finite element method.

The authors are supported by the ANR (Agence Nationale de la Recherche), projects GAOS n° ANR-09-BLAN-0037-03 and Optiform n° ANR-12-BS01-0007-02.

example assume that $\partial\Omega$ is compact, piecewise $\mathcal{C}^{1,+}$ and that Ω satisfies the uniform cone property.

Definition 1.1. For any integer $k \geq 1$, a *k-partition* is a finite set

$$\mathcal{D} = \{D_i : 1 \leq i \leq k\}$$

of open, connected and mutually disjoint subsets of Ω. The D_i's are called the *domains* of the k-partition. The k-partition $\mathcal{D}$ is called *strong* if

$$\mathrm{Int}\left(\overline{\bigcup_{i=1}^{k} D_i}\right) \setminus \partial\Omega = \Omega.$$

The set of all k-partitions is denoted by $\mathfrak{P}_k$.

If we do not want to specify the number of domains, we simply speak of a *partition*.

For any bounded open set $\omega \in \mathbb{R}^2$, the sequence $(\lambda_k(\omega))_{k\geq 1}$ denotes the eigenvalues of the Dirichlet Laplacian on ω, in increasing order and counted with multiplicity. Let us now define the energy of a partition and state the minimization problem we are concerned with.

Definition 1.2. With any k-partition $\mathcal{D} = \{D_i : 1 \leq i \leq k\}$, is associated the *energy*

$$\Lambda_k(\mathcal{D}) = \max_{1\leq i\leq k} \lambda_1(D_i).$$

For any integer $k \geq 1$, we set

$$\mathfrak{L}_k(\Omega) = \inf_{\mathcal{D}\in\mathfrak{P}_k} \Lambda_k(\mathcal{D}). \tag{1}$$

A partition $\mathcal{D} \in \mathfrak{P}_k$ such that $\Lambda_k(\mathcal{D}) = \mathfrak{L}_k(\Omega)$ is called a *minimal k-partition*.

The following existence result for the minimization problem (1) was proved in [7, 9, 8]. Let us notice that similar existence results were previously proved in a more general setting in [6].

Theorem 1.3. *For any integer $k \geq 1$, there exists a minimal k-partition of Ω. Furthermore, minimal partitions are strong.*

Let us now deal with the regularity of the minimal partition.

Definition 1.4. If $\mathcal{D} = \{D_i : 1 \leq i \leq k\}$ is a strong partition, its *boundary set* is defined by

$$N(\mathcal{D}) = \overline{\bigcup_{i=1}^{k} \Omega \cap \partial D_i}.$$

The partition $\mathcal{D}$ is called *regular* if its boundary set satisfies the following properties. First, it is constituted of a finite number of simple regular curves that meet in Ω at *interior singular points* and meet $\partial\Omega$ at *boundary singular points*. Additionally, the curves meeting at an interior singular point form equal angles, and the curves hitting a boundary singular point and $\partial\Omega$ form equal angles.

As proved in [17], we have the following regularity result:

Theorem 1.5. *For any $k \geq 1$, minimal k-partitions are regular (up to zero capacity sets).*

We give additional definitions that help us to describe the topology of a partition.

Definition 1.6. Let $\mathcal{D} = \{D_i : 1 \leq i \leq k\}$ be a strong partition. Two domains D_i and D_j are said to be *neighbors* if $\mathrm{Int}\left(\overline{D_i \cup D_j}\right) \setminus \partial\Omega$ is connected.

A strong partition is called *bipartite* if one can color its domains, using only two colors, in such a way that two neighbors have a different color.

Let us recall some definitions and results from the spectral theory of the Laplacian. They are used throughout the paper. Let u be an eigenfunction for the Dirichlet Laplacian.

Definition 1.7. We call *nodal set* of u the set

$$N(u) = \overline{\{x \in \Omega : u(x) = 0\}}.$$

The connected components of $\Omega \setminus N(u)$ are called the *nodal domains* of u. The number of nodal domains is denoted by $\mu(u)$. The set

$$\{D_i : 1 \leq i \leq \mu(u)\},$$

where the D_i's are the nodal domains of u, is a regular partition of Ω, called the *nodal partition* associated with u.

The following result was proved by Courant (cf. [10]).

Theorem 1.8. *Let $k \geq 1$ and u be an eigenfunction associated with $\lambda_k(\Omega)$, then $\mu(u) \leq k$.*

Following [17], we introduce a new definition.

Definition 1.9. Let $k \geq 1$. An eigenfunction u for the Dirichlet Laplacian associated with $\lambda_k(\Omega)$ is said to be *Courant-sharp* if $\mu(u) = k$.

To give some upper-bound for $\mathfrak{L}_k(\Omega)$, it could be interesting to use k-partitions obtained from eigenfunctions. Thus, we introduce a new spectral element.

Definition 1.10. For $k \geq 1$, $L_k(\Omega)$ is the smallest eigenvalue of the Dirichlet Laplacian that has an eigenfunction with k nodal domains. If there is no such eigenvalue, we set $L_k(\Omega) = +\infty$.

With this notation, Theorem 1.8 reads as the inequality $\lambda_k(\Omega) \leq L_k(\Omega)$. We can now give two results of [17] that link minimal and nodal partitions.

Theorem 1.11. *A minimal partition $\mathcal{D}$ is nodal if, and only if, it is bipartite.*

Theorem 1.12. *For any integer $k \geq 1$,*

$$\lambda_k(\Omega) \leq \mathfrak{L}_k(\Omega) \leq L_k(\Omega).$$

Furthermore, if $\mathcal{L}_k(\Omega) = L_k(\Omega)$ or $\lambda_k(\Omega) = \mathfrak{L}_k(\Omega)$, then

$$\lambda_k(\Omega) = \mathfrak{L}_k(\Omega) = L_k(\Omega),$$

and in this case, any minimal k-partition is nodal.

Let us point out a few consequences of Theorem 1.12.

Remark 1. A nodal partition associated with a Courant-sharp eigenfunction is minimal.

Remark 2. Minimal 2-partitions are nodal. Indeed, let u be an eigenfunction associated with $\lambda_2(\Omega)$. The function u is orthogonal to the eigenspace for $\lambda_1(\Omega)$ and thus has at least two nodal domains. It has at most two nodal domains by Courant's theorem. It is therefore Courant-sharp, which implies that $\mathfrak{L}_2(\Omega) = \lambda_2(\Omega)$ and that any minimal 2-partition of Ω is nodal.

1.2. **Main results.** In this article, we are concerned with the minimal k-partitions of angular sectors. For $0 < \alpha \leq 2\pi$, we set

$$\Sigma_\alpha = \left\{ (\rho\cos\theta, \rho\sin\theta) \ : \ 0 < \rho < 1 \text{ and } -\tfrac{\alpha}{2} < \theta < \tfrac{\alpha}{2} \right\}.$$

This domain is the circular sector of opening α. We denote by $(\lambda_k(\alpha))_{k\geq 1}$ the eigenvalues of the Dirichlet Laplacian on Σ_α, in increasing order and counted with multiplicity. Due to the inclusion of the form domains and the min-max principle, the function $\alpha \mapsto \lambda_k(\alpha)$ is decreasing for any $k \geq 1$.

In Section 2, we recall explicit formulas for the spectrum of the Dirichlet Laplacian on Σ_α and determine the minimal 2-partitions. Furthermore, we establish in Proposition 2 when the k-partition constituted of k equal angular sectors is minimal, according to α and k. In particular, such a partition can never be minimal for $k \geq 6$.

In Section 3, we prove in Proposition 4 that for any k, the minimal k-partition is nodal as soon as α is small enough. In Sections 4-6, we focus on 3-partitions. First, we determine when minimal 3-partitions are nodal (Section 4). Then, Section 5 deals with non nodal symmetric minimal 3-partitions, with some remarks about the particular case $\alpha = \pi/3$. In these two sections, we prove the following result:

Theorem 1.13. *There exists $0 < \alpha_3^1 < \alpha_3^2 < 2\pi$ such that*

- $\mathfrak{L}_3(\Sigma_\alpha) = \lambda_3(\alpha)$, *when* $\alpha \in (0, \alpha_3^1] \cup [\alpha_3^2, 2\pi]$,
- *Let $L_3^{sym}(\alpha)$ be the infimum of the energy $\Lambda_3(\mathcal{D})$ when we minimize among the partitions in $\mathfrak{P}_3$ which are symmetric according to the bissector axis. Then*

$$\lambda_3(\alpha) < \mathfrak{L}_3(\Sigma_\alpha) \leq L_3^{sym}(\alpha) < L_3(\alpha), \quad \forall \alpha \in (\alpha_3^1, \alpha_3^2).$$

This last upper-bound is better than Theorem 1.12 and the improvement is quantified in Figure 12.

Then we use a double covering approach in Section 6. In this way, we refute the seemingly natural conjecture that any domain with an axis of symmetry has a minimal 3-partition that is symmetric, and find some non-symmetric candidates.

Finally we give in Section 7 some negative results for minimal k-partitions when $k = 4, 5, 6$ and give configurations of partitions that are never minimal.

2. Nodal partitions.

2.1. **Explicit eigenmodes.** The eigenvalues and eigenfunctions of the Dirichlet Laplacian in Σ_α can be computed exactly using separation of variables (see e.g. [10, chap. 5, sec. 5]). We recall the results.

Proposition 1. *The eigenmodes $(\lambda_{m,n}(\alpha), u^\alpha_{m,n})$ of the Dirichlet Laplacian on the angular sector Σ_α are given by*

$$\lambda_{m,n}(\alpha) = j^2_{m\frac{\pi}{\alpha},n}, \tag{2}$$

$$u^\alpha_{m,n}(\rho,\theta) = J_{m\frac{\pi}{\alpha}}(j_{m\frac{\pi}{\alpha},n}\rho)\sin(m\pi(\tfrac{\theta}{\alpha} + \tfrac{1}{2})), \tag{3}$$

where $j_{m\frac{\pi}{\alpha},n}$ is the n-th positive zero of the Bessel function of the first kind $J_{m\frac{\pi}{\alpha}}$.

Proof. In polar coordinates, the Laplacian reads

$$-\partial^2_\rho - \frac{1}{\rho}\partial_\rho - \frac{1}{\rho^2}\partial^2_\theta.$$

Let us look for an eigenpair (λ, u) of the Dirichlet Laplacian on Σ_α where $\lambda > 0$ and u is not identically zero. Using a separation of variables, we set $u(\rho,\theta) = \varphi(\rho)\psi(\theta)$, this yields

$$-\frac{\psi''(\theta)}{\psi(\theta)} = \frac{\rho^2}{\varphi(\rho)}\left(\varphi''(\rho) + \frac{1}{\rho}\varphi'(\rho) + \lambda\varphi(\rho)\right).$$

According to the Dirichlet conditions, $\psi(-\frac{\alpha}{2}) = \psi(\frac{\alpha}{2}) = 0$. Therefore there exists an integer $m \geq 1$ such that, up to a constant multiplicative factor,

$$\psi(\theta) = \sin\left(\frac{m\pi}{\alpha}\left(\theta + \frac{\alpha}{2}\right)\right).$$

Then, we get

$$\varphi''(\rho) + \frac{1}{\rho}\varphi'(\rho) + \left(\lambda - \frac{m^2\pi^2}{\alpha^2\rho^2}\right)\varphi(\rho) = 0.$$

If we set

$$\nu = \frac{\pi}{\alpha}, \quad \lambda = \omega^2, \quad t = \omega\rho, \quad f(t) = \varphi(\rho),$$

we recognize the Bessel differential equation

$$f''(t) + \frac{1}{t}f'(t) + \left(1 - \frac{m^2\nu^2}{t^2}\right)f(t) = 0.$$

The function u is assumed to be in $H^1(\Sigma_\alpha)$ and to satisfy the Dirichlet boundary condition. This implies that f is proportional to the Bessel function of the first kind $J_{m\nu}$ and that ω is a zero of $J_{m\nu}$.

We have obtained a family of eigenmodes $(\lambda_{m,n}(\alpha), u^\alpha_{m,n})$ indexed by $m \geq 1$ and $n \geq 1$. More precisely, we have the expressions (3)–(2). We can check that the set $\{u^\alpha_{m,n}\}_{m,n}$ is orthogonal and spans $L^2(\Sigma_\alpha)$. Therefore there is no other eigenvalue. □

Corollary 1. *For any $k \geq 2$ and $\alpha \in (0, 2\pi]$, we have the first estimate*

$$\lambda_k(\alpha) \leq \mathfrak{L}_k(\alpha) \leq L_k(\Sigma_\alpha) \leq \inf\{\lambda_{m,n}(\alpha) : mn = k\}.$$

Proof. It is enough to use Theorem 1.12, Proposition 1 and to notice that for any $m \geq 1, n \geq 1$, and $\alpha \in (0, 2\pi]$, the eigenfunction $u^\alpha_{m,n}$ has mn nodal domains. □

In Figure 1 are plotted some eigenvalues $\lambda_{m,n}(\alpha)$ for $1 \leq m \leq 7$, $1 \leq n \leq 4$, and $\alpha \in (0, 2\pi]$. These eigenvalues are computed with the MATLAB software and the *fsolve* command to determine the zero $j_{m\nu,n}$ of the implemented Bessel functions.

2.2. **Minimal nodal partition.**

Proposition 2. *For $2 \leq k \leq 5$, we define*

$$\alpha_k^2 = \inf\{\alpha \in (0, 2\pi] : \lambda_{k,1}(\alpha) < \lambda_{1,2}(\alpha)\}.$$

Then for any $\alpha \in [\alpha_k^2, 2\pi]$, the nodal partition associated with $u^\alpha_{k,1}$ is a minimal k-partition and we have

$$\mathfrak{L}_k(\Sigma_\alpha) = \lambda_{k,1}(\alpha).$$

For $2 \leq k \leq 5$ and $\alpha \in (\alpha_k^2, 2\pi]$, the minimal k-partition consists then of k angular sectors with the same aperture.

For $k \geq 6$, any k-partition constituted of k angular sectors is never minimal.

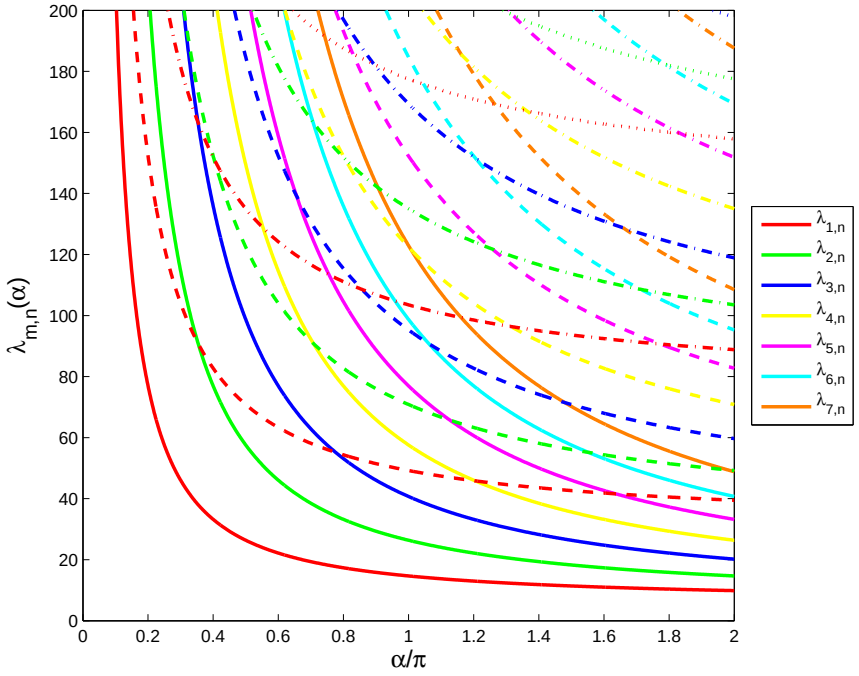

FIGURE 1. $\lambda_{m,n}(\alpha)$ vs. α/π for $1 \leq m \leq 7$, $1 \leq n \leq 4$.

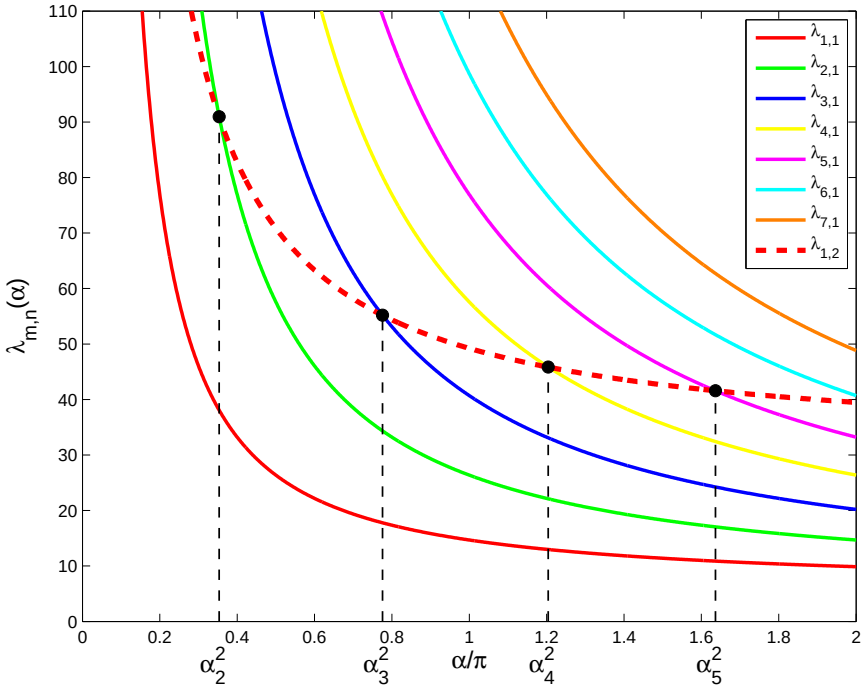

FIGURE 2. $\lambda_{m,1}(\alpha)$ vs. α/π for $1 \leq m \leq 7$, compared with $\lambda_{1,2}(\alpha)$.

Proof. Let us use the expression of the eigenvalues given in (2) and compare $\lambda_{m,1}(\alpha)$ with $\lambda_{1,2}(\alpha)$, computed with the MATLAB software, in Figure 2.

We have

$$\lambda_{k,1}(2\pi) < \lambda_{1,2}(2\pi) \qquad \text{for } k = 2, \dots, 5.$$

By continuity of $\alpha \mapsto \lambda_{k,1}(\alpha)$, the real number α_k^2 is well defined for $2 \leq k \leq 5$, and for any $\alpha \in (\alpha_k^2, 2\pi]$, we have

$$\lambda_{k,1}(\alpha) < \lambda_{1,2}(\alpha) \qquad \text{for } k = 2, \dots, 5.$$

Using the definition of α_k^2, we have

$$\lambda_k(\alpha) = \lambda_{k,1}(\alpha), \qquad \forall \alpha \in (\alpha_k^2, 2\pi].$$

Since $u_{k,1}^\alpha$ has k nodal domains, it is Courant-sharp and its nodal partition, composed of k equal angular sectors, is minimal according to Remark 1.

For $k \geq 6$, we observe that $\lambda_{k,1}(\alpha) > \lambda_{1,2}(\alpha)$ for any $\alpha \in (0, 2\pi]$. Then $\lambda_{k,1}(\alpha) > \lambda_k(\alpha)$, the eigenfunction $u_{k,1}^\alpha$ is not Courant-sharp, and its nodal partition is not minimal.

Still assuming $k \geq 6$, let us prove by contradiction that a k-partition $\mathcal{D}_k = (D_1, \dots, D_k)$ with D_i angular sector cannot be minimal. Let us assume that it is minimal. Then the aperture for each sector must be the same, otherwise we could decrease the energy by increasing some angles and decreasing others. The partition $\mathcal{D}_k$ is therefore nodal, associated with $u_{k,1}$, and thus not minimal. □

2.3. **Minimal 2-partition.** According to Remark 2, we know that

$$\mathfrak{L}_2(\Sigma_\alpha) = \lambda_2(\alpha), \qquad \forall 0 < \alpha \leq 2\pi.$$

Furthermore a minimal 2-partition is given by the nodal partition associated with $\lambda_2(\alpha)$.

To be more precise, for $\alpha < \alpha_2^2$, $\lambda_2(\alpha)$ is simple and equal to $\lambda_{1,2}(\alpha)$ and for $\alpha > \alpha_2^2$, $\lambda_2(\alpha)$ is simple and equal to $\lambda_{2,1}(\alpha)$. For $\alpha < \alpha_2^2$ and $\alpha > \alpha_2^2$, there is a unique minimal 2-partition, given by the nodal domains of $u_{1,2}^\alpha$ and $u_{2,1}^\alpha$ respectively. Thus we have

Proposition 3.

$$\mathfrak{L}_2(\Sigma_\alpha) = \begin{cases} \lambda_{1,2}(\alpha) & \text{for } 0 < \alpha \leq \alpha_2^2, \\ \lambda_{2,1}(\alpha) & \text{for } \alpha_2^2 \leq \alpha \leq 2\pi. \end{cases}$$

Figure 3 gives the unique minimal 2-partition when $\alpha \neq \alpha_2^2$.

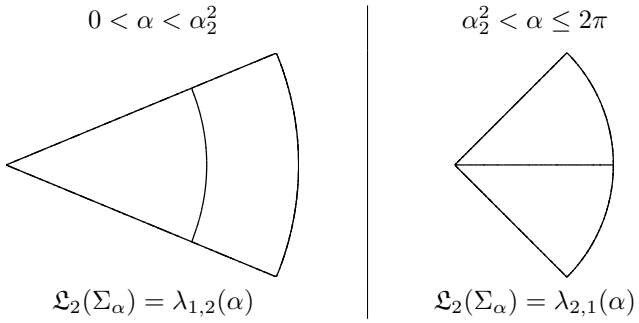

FIGURE 3. Minimal 2-partition on Σ_α.

We notice that the eigenfunction $u^\alpha_{1,2}$ is symmetric with respect to the axis $\{y = 0\}$ while $u^\alpha_{2,1}$ is antisymmetric.

Let us determine α_2^2 and the associated eigenvalue using (2). We set $\nu = \pi/\alpha_2^2$ and $j = j_{\nu,2} = j_{2\nu,1}$. The pair (ν, j) is a solution of the (nonlinear) system

$$\left\{ \begin{array}{rcl} J_\nu(j) & = & 0, \\ J_{2\nu}(j) & = & 0. \end{array} \right.$$

We can solve this system numerically by any iterative method. The initial values must be chosen so that j is indeed the second zero of J_ν and the first of $J_{2\nu}$. In practice we find approximations of j and ν thanks to Figure 2 and use them as initial values. We get

$$\begin{array}{rcl} \alpha_2^2 & \simeq & 0.3541\ \pi \simeq 1.1125, \\ \lambda_2(\alpha_2^2) & \simeq & 90.7745. \end{array}$$

For $\alpha = \alpha_2^2$, $\lambda_2(\alpha) = \lambda_{1,2}(\alpha) = \lambda_{2,1}(\alpha)$ has a two-dimensional eigenspace and the nodal domains of any nonzero linear combination of $u^\alpha_{1,2}$ and $u^\alpha_{2,1}$ give a minimal 2-partition (see Figure 4). The eigenfunctions were computed by using the Finite Element Library MÉLINA [19]. We then used the MATLAB software to compute linear combinations of two eigenfunctions and to catch the nodal lines of the new function.

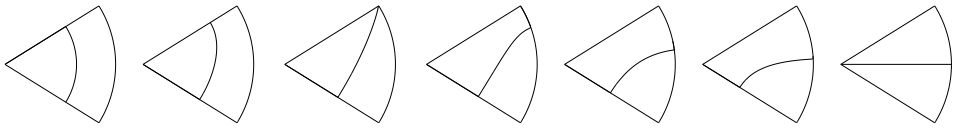

FIGURE 4. Minimal 2-partitions obtained as nodal partitions of $(1-t)u^\alpha_{1,2} + tu^\alpha_{2,1}$, $\alpha = \alpha_2^2$.

3. **Minimal partition for small angles.** For sufficiently small angles, the minimal k-partition is nodal as explained in the following proposition.

Proposition 4. *Let $k \geq 2$, we define*

$$\alpha_k^1 := \inf\{\alpha \in (0, 2\pi] \ : \ \lambda_{1,k}(\alpha) \geq \lambda_{2,1}(\alpha)\}. \tag{4}$$

Then $\alpha_k^1 > 0$ and for any $0 < \alpha < \alpha_k^1$, there is a unique minimal k-partition of Σ_α, which is nodal, and more precisely consists of the nodal sets of $u^\alpha_{1,k}$.

Proof. Using [12, 20], we determine the asymptotic expansion of the n-th zero $j_{\tilde\nu,n}$ of the Bessel function $J_{\tilde\nu}$ for large $\tilde\nu$:

$$j_{\tilde\nu,n} = \tilde\nu - 2^{-1/3} a_n \tilde\nu^{1/3} + \mathcal{O}\left(\tilde\nu^{-1/3}\right).$$

Here a_n is the n-th negative zero of the Airy function Ai. Together with (2) and the relation $\tilde\nu = m\pi/\alpha$, this yields an asymptotic expansion for the eigenvalues :

$$\lambda_{m,n}(\alpha) = \frac{m^2\pi^2}{\alpha^2} + 2^{2/3}|a_n| \left(\frac{m\pi}{\alpha}\right)^{4/3} + \mathcal{O}\left(\alpha^{-2/3}\right). \tag{5}$$

Let $k \geq 2$ be an integer. The asymptotic expansion (5) implies that for α small enough, $\lambda_{1,k}(\alpha) < \lambda_{2,1}(\alpha)$. Then the real number α_k^1 defined by relation (4) is

strictly positive. For $\alpha \in (0, \alpha_k^1)$, we have $\lambda_{1,k}(\alpha) < \lambda_{2,1}(\alpha)$ and therefore the first k eigenvalues of the Dirichlet Laplacian on Σ_α are $\lambda_{1,1}(\alpha), \dots, \lambda_{1,k}(\alpha)$. These eigenvalues are simple. Let $u_{1,1}^\alpha, \dots, u_{1,k}^\alpha$ be the associated eigenfunctions defined by (3). The eigenfunction $u_{1,k}^\alpha$ has k nodal domains and therefore is Courant-sharp. According to Theorem 1, the nodal partition associated with $u_{1,k}^\alpha$ is minimal. Furthermore, the eigenspace associated with $\lambda_{1,k}^\alpha$ has dimension 1 and thus this partition is unique. □

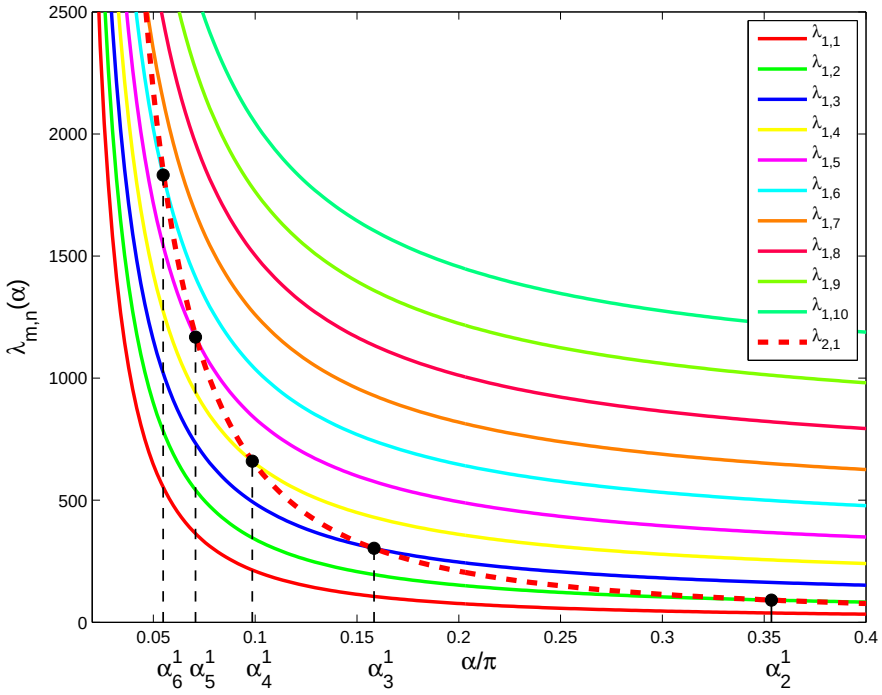

FIGURE 5. $\lambda_{1,k}(\alpha)$ vs. α/π for $1 \le k \le 10$, compared with $\lambda_{2,1}(\alpha)$.

Figure 5 gives the first ten eigenvalues $\lambda_{1,k}(\alpha)$ compared with $\lambda_{2,1}(\alpha)$ and shows the critical angles α_k^1. We have

$$\begin{aligned} \alpha_2^1 &= \alpha_2^2, \\ \alpha_k^1 &< \alpha_k^2, \qquad \text{for } k = 3, \dots, 5. \end{aligned}$$

Then we deduce from Propositions 2 and 4 the estimate of the energy of a minimal k-partition.

Proposition 5. *For any* $2 \le k \le 5$,

$$\begin{aligned} \mathfrak{L}_k(\Sigma_\alpha) &= \lambda_k(\alpha), && \forall \alpha \in (0, \alpha_k^1] \cup [\alpha_k^2, 2\pi], \\ \lambda_k(\alpha) < \mathfrak{L}_k(\Sigma_\alpha) &< L_k(\alpha), && \forall \alpha \in (\alpha_k^1, \alpha_k^2). \end{aligned}$$

Remark 3. Using the asymptotic expansion, we deduce that $\lambda_{1,k}(\alpha) \le \lambda_{k,1}(\alpha)$ as soon as α is small enough. Let k be a prime number, we define

$$\beta_k = \inf\{\alpha \in (0, 2\pi] \ : \lambda_{1,k}(\alpha) \ge \lambda_{k,1}(\alpha)\}. \tag{6}$$

Then , we have $\beta_2 = \alpha_2^1 = \alpha_2^2$ and

$$L_k(\Sigma_\alpha) \leq \begin{cases} \lambda_{1,k}(\alpha) & \text{if } 0 < \alpha \leq \beta_k, \\ \lambda_{k,1}(\alpha) & \text{if } \beta_k \leq \alpha \leq 2\pi. \end{cases}$$

4. **Minimal nodal 3-partition.** This section is devoted to the proof of the first point of Theorem 1.13.

As in the case of the 2-partition, we estimate numerically the transition angles α_3^1, α_3^2, β_3:

$$\begin{array}{rcllrcl} \alpha_3^1 & \simeq & 0.1579\ \pi \simeq 0.4961, & & \lambda_3(\alpha_3^1) & \simeq & 303.9139, \\ \alpha_3^2 & \simeq & 0.7761\ \pi \simeq 2.4382, & & \lambda_3(\alpha_3^2) & \simeq & 55.1671, \\ \beta_3 & \simeq & 0.3533\ \pi \simeq 1.1098, & & L_3(\beta_3) & \simeq & 163.3786. \end{array}$$

Proposition 5 and Remark 3 give estimates for $\mathfrak{L}_3(\Sigma_\alpha)$ illustrated in Figure 6:

- for $0 < \alpha \leq \alpha_3^1$, $\mathfrak{L}_3(\Sigma_\alpha) = \lambda_3(\alpha) = \lambda_{1,3}(\alpha)$,
- for $\alpha_3^1 < \alpha \leq \beta_3$, $\lambda_{2,1}(\alpha) = \lambda_3(\alpha) < \mathfrak{L}_3(\Sigma_\alpha) < L_3(\Sigma_\alpha) = \lambda_{1,3}(\alpha)$,
- for $\beta_3 \leq \alpha \leq \beta_2$, $\lambda_{2,1}(\alpha) = \lambda_3(\alpha) < \mathfrak{L}_3(\Sigma_\alpha) < L_3(\Sigma_\alpha) = \lambda_{3,1}(\alpha)$,
- for $\beta_2 \leq \alpha < \alpha_3^2$, $\lambda_{1,2}(\alpha) = \lambda_3(\alpha) < \mathfrak{L}_3(\Sigma_\alpha) < L_3(\Sigma_\alpha) = \lambda_{3,1}(\alpha)$,
- for $\alpha_3^2 \leq \alpha \leq 2\pi$, $\mathfrak{L}_3(\Sigma_\alpha) = \lambda_3(\alpha) = \lambda_{3,1}(\alpha)$.

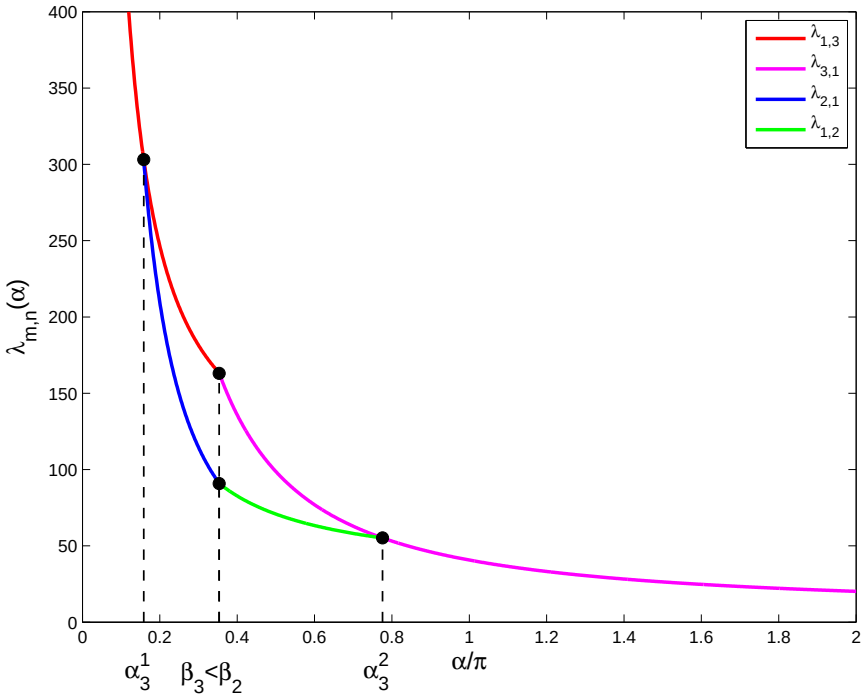

FIGURE 6. Lower and upper bounds for $\mathfrak{L}_3(\Sigma_\alpha)$.

If $\alpha \leq \alpha_3^1$ or $\alpha \geq \alpha_3^2$, the eigenvalue $\lambda_3(\alpha)$ has a Courant-sharp eigenfunction. According to Remark 1, $\mathfrak{L}_3(\Sigma_\alpha) = \lambda_3(\alpha)$ and the minimal 3-partition is nodal, given by the nodal sets of an eigenfunction associated with $\lambda_3(\alpha)$. On the other hand, if $\alpha_3^1 < \alpha < \alpha_3^2$, no minimal 3-partition is nodal. Table 1 gives the nodal

partition associated with the third eigenfunction. We notice that the eigenfunctions $u^\alpha_{1,3}$ and $u^\alpha_{3,1}$ are symmetric with respect to the axis $\{y = 0\}$.

$0 < \alpha \leq \alpha^1_3$	$\alpha^1_3 < \alpha < \alpha^1_2$	$\alpha^1_2 < \alpha < \alpha^2_3$	$\alpha^1_3 \leq \alpha \leq 2\pi$
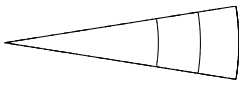	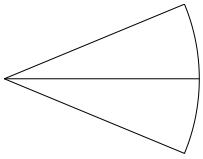	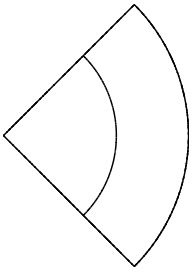	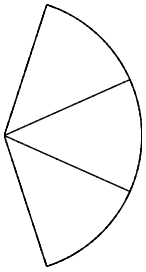
$\mathfrak{L}_3(\Sigma_\alpha) = \lambda_{1,3}(\alpha)$ *minimal 3-partition*	$\lambda_{2,1}(\alpha) < \mathfrak{L}_3(\Sigma_\alpha)$	$\lambda_{1,2}(\alpha) < \mathfrak{L}_3(\Sigma_\alpha)$	$\mathfrak{L}_3(\Sigma_\alpha) = \lambda_{3,1}(\alpha)$ *minimal 3-partition*

TABLE 1. Nodal partition associated with $\lambda_3(\alpha)$ on Σ_α.

Let us now look at the transition angles α^1_3 and α^2_3. For such angles, the minimal 3-partition is no more unique.

Figure 7 represents the nodal partitions of some linear combination $(1-t)u^\alpha_{1,3} + tu^\alpha_{2,1}$ for $\alpha = \alpha^1_3$. There is a transition between a 2-partition and a 3-partition. When we have a 3-partition, it is a minimal one since the eigenfunction is associated with $\lambda_3(\alpha)$ and then Courant-sharp (see Remark 1). Notice that the function $u^\alpha_{1,3}$ is symmetric with respect to the y-axis whereas the function $u^\alpha_{2,1}$ is antisymmetric. Thus, by considering linear combinations, we break the symmetry of the 3-partition and exhibit some minimal 3-partitions which are non symmetric.

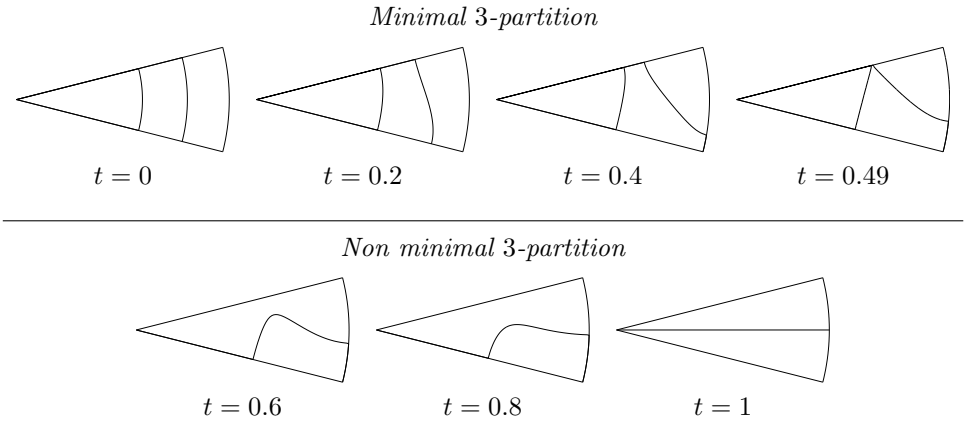

FIGURE 7. Nodal partitions of $(1-t)u^\alpha_{1,3} + tu^\alpha_{2,1}$, $\alpha = \alpha^1_3$.

The following proposition gives information about the transition in the linear combinations between 2-partition and 3-partition.

Proposition 6. *There are eigenfunctions associated with $\lambda_3(\alpha^1_3)$ whose nodal set has a boundary singular point with two nodal lines which hit at this point. The polar*

coordinates of this boundary singular point is either $(\rho_c, \alpha_3^1/2)$ *or* $(\rho_c, -\alpha_3^1/2)$ *with* $\rho_c \simeq 0.6558$.

Proof. We recall that

$$\lambda_3(\alpha_3^1) = \lambda_{1,3}(\alpha_3^1) = \lambda_{2,1}(\alpha_3^1).$$

We set

$$\nu = \frac{\pi}{\alpha_3^1}, \qquad j = j_{\nu,3} = j_{2\nu,1}.$$

Any associated eigenfunction is of the form

$$u(\rho,\theta) = aJ_\nu(j\rho)\cos(\nu\theta) + bJ_{2\nu}(j\rho)\sin(2\nu\theta),$$

where a and b are coefficients to be determined. It can be factorized as

$$u(\rho,\theta) = J_{2\nu}(j\rho)\cos(\nu\theta)\left(a\frac{J_\nu(j\rho)}{J_{2\nu}(j\rho)} + 2b\sin(\nu\theta)\right).$$

Let us define

$$v(\rho,\theta) = a\frac{J_\nu(j\rho)}{J_{2\nu}(j\rho)} + 2b\sin(\nu\theta).$$

We are looking for values of a and b for which v has a zero that is also a singular point. The equation $\nabla v(\rho,\theta) = 0$ can be solved and yields

$$\begin{cases} \theta_c &= \pm\alpha_3^1/2, \\ \rho_c &\simeq 0.6558. \end{cases}$$

Thanks to the equation $v(\theta_c, \rho_c) = 0$, we then find a and b up to a common multiplicative factor. □

Similarly, Figure 8 gives the nodal partition associated with the linear combination $(1-t)u_{1,2}^\alpha + tu_{3,1}^\alpha$ for $\alpha = \alpha_3^2$. In this case, the functions $u_{1,2}$ and $u_{3,1}$ are both symmetric with respect to the y-axis. Then any linear combination satisfies this symmetry too. As previously, we observe a transition between a 2-partition

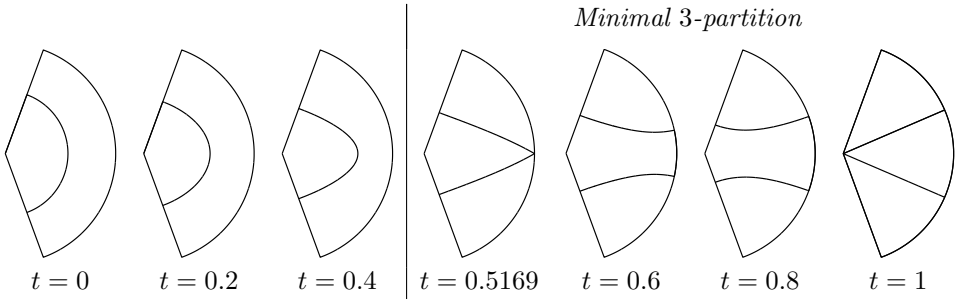

FIGURE 8. Nodal partition of $(1-t)u_{1,2}^\alpha + tu_{3,1}^\alpha$, $\alpha = \alpha_3^2$.

and a 3-partition. When we have a 3-partition, it is still a minimal one. We can characterize the transition between 2-partition and 3-partition:

Proposition 7. *There are eigenfunctions associated with* $\lambda_3(\alpha_3^2)$ *for which the point of coordinates* $(1,0)$ *is a boundary singular point. Two nodal lines meet at this point.*

Proof. This proposition is proved in the same way than Proposition 6. □

5. **Minimal symmetric 3-partitions.** In this section, we prove the second point of Theorem 1.13. We restrict ourselves to symmetric 3-partitions and analyze the minimization problem with that additional condition. We study each possible symmetric configuration and exhibit better upper-bounds for the energy $\mathfrak{L}_3(\Sigma_\alpha)$ and also give new candidates to be minimal 3-partitions. This approach was used in [5] to catch symmetric candidates for the square and the disk.

Looking at nodal minimal 3-partitions obtained in Section 4, we observe that for any $\alpha \in (0, \alpha_3^1] \cup [\alpha_3^2, 2\pi]$, there exists a symmetric minimal 3-partition. Now, we exhibit symmetric candidates to be minimal symmetric 3-partitions for $\alpha \in (\alpha_3^1, \alpha_3^2)$. We refer to [5] to explain the possible symmetric configurations. Using the Euler formula (cf. [14]), there are only three configurations, represented in Figure 9, for the minimal 3-partition when $\alpha_3^1 < \alpha < \alpha_3^2$:

(a) The 3-partition has one interior singular point X_0, which is necessarily on the symmetry axis.
(b) The 3-partition has two interior singular points X_0, X_1 and no boundary singular point.
(c) The 3-partition has two interior singular points and two boundary singular points. Moreover $\partial D_1 \cap \partial D_2$ consists of two curves, each one joining one boundary singular point to one interior singular point.

In configurations (b) and (c), the interior singular points X_0, X_1 (and boundary singular points for case (c)) are either on the symmetry axis, or symmetric to each other.

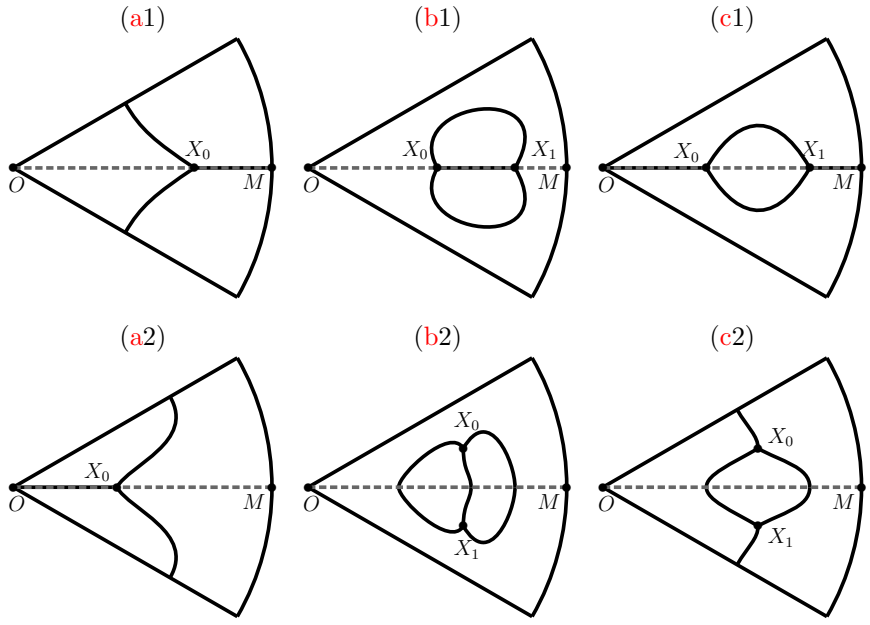

FIGURE 9. Configuration of the non bipartite symmetric minimal 3-partition.

5.1. **Partitions with one interior singular point.** Let us first consider configurations of type (a). To catch such configuration, it is enough to deal with the

half-domain $\Sigma_\alpha^+ = \Sigma_\alpha \cap \{y > 0\}$ and look at 2-partitions on this half-domain. The main advantage is that the minimal 2-partitions are nodal; to determine them, it is enough to compute the second eigenfunction. The unknown parameter is the position of the singular point X_0^α. Thus we compute the second eigenvector of the Neumann-Dirichlet and Dirichlet-Neumann Laplacian on Σ_α^+ and move the singular point all along the axis $\{y = 0\}$; we denote by x_α the abscissa of the singular point X_0^α and by $\lambda_2^{ND}(x_\alpha)$ and $\lambda_2^{DN}(x_\alpha)$ the second eigenvalue of the Neumann-Dirichlet and Dirichlet-Neumann Laplacian respectively (see Figures 9(a1) and 9(a2)):

Neumann-Dirichlet

$$\text{(a1)} \quad \begin{cases} -\Delta\varphi = \lambda\varphi & \text{in } \Sigma_\alpha^+, \\ \partial_{\mathbf{n}}\varphi = 0 & \text{on } [O, X_0^\alpha], \\ \varphi = 0 & \text{elsewhere,} \end{cases}$$

Dirichlet-Neumann

$$\text{(a2)} \quad \begin{cases} -\Delta\varphi = \lambda\varphi & \text{in } \Sigma_\alpha^+, \\ \partial_{\mathbf{n}}\varphi = 0 & \text{on } [X_0^\alpha, M], \\ \varphi = 0 & \text{elsewhere.} \end{cases}$$

For each mixed problem, the nodal line of the second eigenvector meets the axis $\{y = 0\}$ at a point of abscissa denoted by $y^{ND}(x_\alpha)$ and $y^{DN}(x_\alpha)$ respectively. The choice of the interior singular point X_0^α gives a 3-partition after symmetrization if and only if

- $y^{ND}(x_\alpha) \geq x_\alpha$ in the Neumann-Dirichlet case,
- $y^{DN}(x_\alpha) \leq x_\alpha$ in the Dirichlet-Neumann case.

We compute the eigenmodes associated with the mixed problems (a1)–(a2) by using the Finite Element Library MÉLINA [19]. Figure 10 gives examples of nodal partitions for several values of x_α. The Dirichlet condition on the boundary is represented in blue line and the Neumann condition in red dotted line. The nodal line is plotted in black. For the Neumann-Dirichlet configuration (see Figure 10(a)), we obtain a 2-partition after symmetrization if x_α is too large. If x_α is such that $x_\alpha < y^{ND}(x_\alpha)$, we obtain a 3-partition whose energy can be reduced by removing the Dirichlet line $(Y^{ND}(x_\alpha), X_0^\alpha)$ (where $Y^{ND}(x_\alpha)$ is the point of coordinates $(y^{ND}(x_\alpha), 0)$) in this subdomain of the partition. We can make a similar analysis in the Dirichlet-Neumann case (see Figure 10(b)).

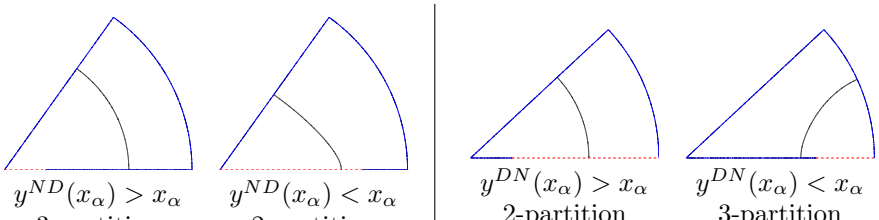

(a) Neumann-Dirichlet condition.

(b) Dirichlet-Neumann condition.

FIGURE 10. Examples of nodal partition for the mixed problems.

Since the function $x \mapsto \lambda_2^{ND}(x)$ is decreasing with x and $x \mapsto \lambda_2^{DN}(x)$ is increasing with x, the optimal singular points are:

$$x_\alpha^{ND} = \max\{x_\alpha : y^{ND}(x_\alpha) \geq x_\alpha\}, \qquad x_\alpha^{DN} = \min\{x_\alpha : y^{DN}(x_\alpha) \leq x_\alpha\}. \tag{7}$$

For numerical simulations, we use the discretization

$$\alpha \in \{\tfrac{k}{100}\pi, 16 \leq k \leq 77\} \qquad \text{and} \qquad x_\alpha \in \{\tfrac{j}{100}, 0 \leq j \leq 100\}.$$

We denote by $\tilde{x}_\alpha^{ND}$ and $\tilde{x}_\alpha^{DN}$ the singular points defined by (7) for a discretization $x_\alpha \in \{\frac{j}{100}, 0 \leq j \leq 100\}$. Figure 11 represents these singular points according to α.

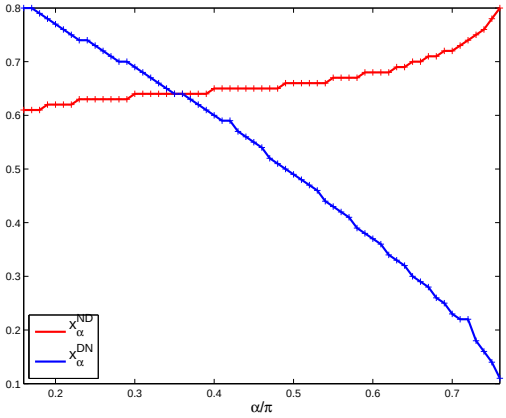

FIGURE 11. $\tilde{x}_\alpha^{ND}$ and $\tilde{x}_\alpha^{DN}$ vs. $\alpha \in \{k\pi/100, 16 \leq k \leq 77\}$.

The 3-partitions obtained after symmetrization give upper-bounds for $\mathfrak{L}_3(\alpha)$ as illustrated in Figure 12. We observe that the energy for the Neumann-Dirichlet Laplacian (green curve) is smaller than the one obtained with the Dirichlet-Neumann Laplacian (cyan curve) and smaller than $L_3(\alpha)$ (red and pink curves). Thus using Theorem 1.12, we deduce

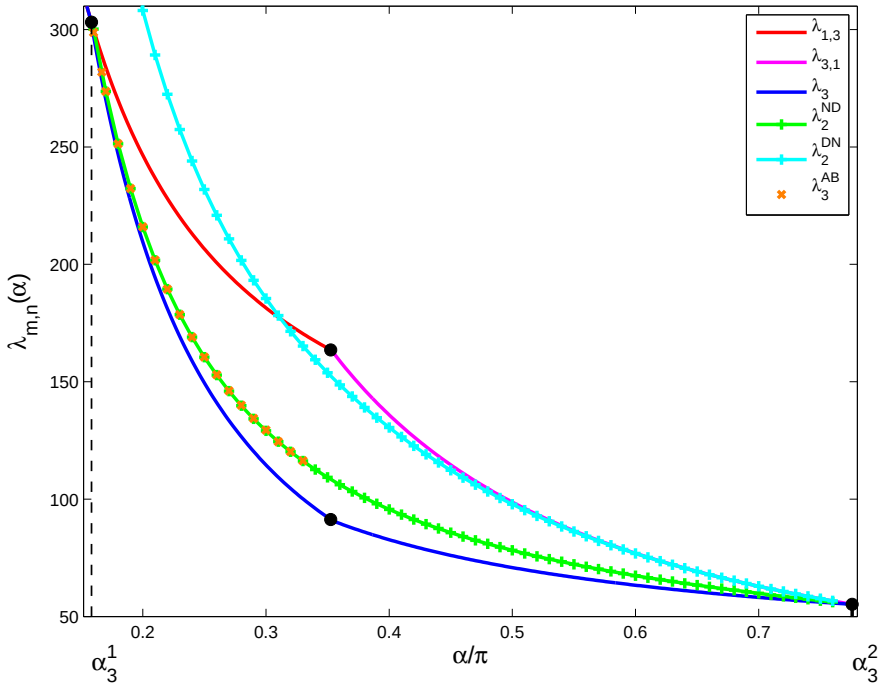

FIGURE 12. Upper-bound of $\mathfrak{L}_3(\Sigma_\alpha)$ using symmetric partitions.

Proposition 8. *For any* $\alpha \in (\alpha_3^1, \alpha_3^2)$,

$$\lambda_3(\alpha) < \mathfrak{L}_3(\Sigma_\alpha) \leq L_3^{sym}(\alpha) < L_3(\alpha),$$

with $L_3^{sym}(\alpha) := \min(\lambda_2^{DN}(x_\alpha^{DN}), \lambda_2^{ND}(x_\alpha^{ND})) = \lambda_2^{ND}(x_\alpha^{ND})$.

Looking at Figure 12, this new upper-bound $L_3^{sym}(\alpha)$ (represented by the green curve) is much more accurate than the previously known upper-bound $L_3(\alpha)$ represented by the red and pink curves. Figure 13 gives examples of minimal symmetric 3-partitions of type (a) for several angles. We denote by $\mathcal{D}_\alpha^{sym}$ the best candidate obtained like this.

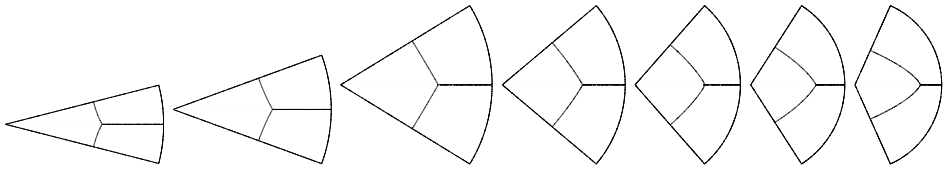

FIGURE 13. Best candidates for symmetric 3-partition.

5.2. **Partitions with two interior singular points.** We have now to deal with the other configurations (b) and (c). Then, as illustrated in Figure 9, the two interior singular points X_0 and X_1 are either on the axis $\{y = 0\}$, or symmetric to each other. Their coordinates are therefore:

1. $X_0 = (x_0, 0)$ and $X_1 = (x_1, 0)$ in case (b1) or (c1),
2. $X_0 = (x_0, y_0)$ and $X_1 = (x_0, -y_0)$ in case (b2) or (c2).

Let us first rule out configurations (b2) and (c2):

Lemma 5.1. *Let* $\alpha \in (\alpha_3^1, \alpha_3^2)$ *and* $\mathcal{D}_\alpha$ *be a minimal* 3*-partition. We assume that this partition is symmetric with respect to the* y*-axis. Then the interior singular points are necessarily on the axis* $\{y = 0\}$.

Proof. This is clear for configuration of type (a) and we have used this property previously. Let us now assume that the partition $\mathcal{D}_\alpha$ is of type (b2) or (c2). Then, since $\mathcal{D}_\alpha^+ = \mathcal{D}_\alpha \cap \{y > 0\}$ is a 3-partition with Neumann condition on the symmetry axis $\{y = 0\}$, we infer, by the min-max principle,

$$\Lambda_3(\mathcal{D}_\alpha) \geq \lambda_3^N(\alpha),$$

where $\lambda_3^N(\alpha)$ is the third eigenvalue on Σ_α^+ with Neumann condition on $\{y = 0\}$ and Dirichlet condition elsewhere. But $\lambda_3^N(\alpha) = \lambda_{1,3}(\alpha)$ if $\alpha_3^1 < \alpha \leq \beta_3$ and $\lambda_3^N(\alpha) = \lambda_{3,1}(\alpha)$ if $\beta_3 \leq \alpha < \alpha_3^2$, that is to say

$$\lambda_3^N(\alpha) = L_3(\alpha), \qquad \forall \alpha \in (\alpha_3^1, \alpha_3^2).$$

Using Proposition 8 and Figure 12, we observe that for any $\alpha \in (\alpha_3^1, \alpha_3^2)$, we find a symmetric 3-partition $\mathcal{D}_\alpha^{sym}$ of type (a1) such that

$$\Lambda_3(\mathcal{D}_\alpha^{sym}) < L_3(\alpha) \leq \Lambda_3(\mathcal{D}_\alpha).$$

Thus $\mathcal{D}_\alpha$ cannot be a minimal 3-partition. □

We have then reduced the study to configurations (b1) and (c1). The associated mixed problems read

Neumann-Dirichlet-Neumann

$$\text{(b1)}\quad \begin{cases} -\Delta\varphi = \lambda\varphi & \text{in } \Sigma_\alpha^+, \\ \partial_{\mathbf{n}}\varphi = 0 & \text{on } [O, X_0^\alpha] \cup [X_1^\alpha, M], \\ \varphi = 0 & \text{elsewhere,} \end{cases}$$

Dirichlet-Neumann-Dirichlet

$$\text{(c1)}\quad \begin{cases} -\Delta\varphi = \lambda\varphi & \text{in } \Sigma_\alpha^+, \\ \partial_{\mathbf{n}}\varphi = 0 & \text{on } [X_0^\alpha, X_1^\alpha], \\ \varphi = 0 & \text{elsewhere.} \end{cases}$$

Using the results of Subsection 5.1 for the configuration (a), we can restrict the possible critical points for configuration (c1):

Proposition 9. *Let $\mathcal{D} = (D_1, D_2, D_3)$ be a symmetric 3-partition of type (c1) with the interior singular points X_0^α and X_1^α of coordinates $(x_0, 0)$ and $(x_1, 0)$. We assume either $x_0 < x_1 \leq x_\alpha^{ND}$, or $x_\alpha^{DN} \leq x_0 < x_1$. Then this partition cannot be minimal.*

Proof. We assume that $x_0 < x_1 < x_\alpha^{ND}$ and that $D_1 \subset \{y > 0\}$ and $D_3^+ = D_3 \cap \{y > 0\} \neq \emptyset$. Then the partition $\mathcal{D}^+ = (D_1, D_3^+)$ satisfies the Dirichlet-Neumann-Dirichlet problem (c1) and we have then, by the min-max principle,

$$\Lambda_3(\mathcal{D}) \geq \lambda_2^{DND}(x_0, x_1),$$

with $\lambda_2^{DND}(x_0, x_1)$ the second eigenvalue of the Dirichlet-Neumann-Dirichlet Laplacian (c1) on Σ_α^+. By monotonicity due to the Dirichlet condition and since $x_0 < x_1 \leq x_\alpha^{ND}$, we have

$$\lambda_2^{DND}(x_0, x_1) > \lambda_2^{ND}(x_1) \geq \lambda_2^{ND}(x_\alpha^{ND}) = L_3^{sym}(\alpha) \geq \mathfrak{L}_3(\alpha).$$

Thus the partition $\mathcal{D}$ cannot be minimal.

The proof is similar if we assume $x_\alpha^{DN} \leq x_0 < x_1$. □

Figure 11 gives an approximation at 1/100 for x_α^{ND} and x_α^{DN} and thus the location for possible interior singular points for configuration (c1).

When we search for candidates of type (b1) or (c1) numerically, we use the discretization

$$\alpha \in \{\tfrac{k}{100}\pi, 16 \leq k \leq 77\}, \quad X_k^\alpha = (x_k^\alpha, 0), \quad x_k^\alpha \in \{\tfrac{j}{100}, 0 \leq j \leq 100\}, \quad k = 0, 1.$$

As in [5] for the square and the disk, the second eigenfunction associated with these mixed problems never produces a configuration of type (b) or (c). Then the mixed Neumann-Dirichlet problem provides the best symmetric candidates for any $\alpha \in (\alpha_3^1, \alpha_3^2)$.

This concludes the proof of Theorem 1.13.

5.3. **Angular sector of opening $\alpha = \pi/3$.** Let us analyze more specifically the case $\alpha = \pi/3$. Using the approach developed in Subsection 5.1, the best candidate obtained is represented in Figure 14 with $\tilde{x}_{\pi/3}^{ND} = 0.64$ (we recall that for the numerics, $x_\alpha \in \{k/100, 0 \leq k \leq 100\}$). It seems that the nodal lines are straight lines. This is compatible with the equal angle properties: At the interior singular point, the nodal lines have to meet with angle $2\pi/3$ whereas the nodal lines meet the boundary at right angles.

Let us try to understand some properties of such a partition. We reproduce this 3-partition of $\Sigma_{\pi/3}$ by rotation of $\pm\pi/3$ and $\pm 2\pi/3$ to tile the disk. Figure 15 represents this tiling of the disk. Let us compare the areas of the subdomains $(\Omega_1, \Omega_2, \Omega_3)$ of the partition of $\Sigma_{\pi/3}$, assuming that the nodal lines are straight lines. We denote by A the interior singular point of coordinates $(L, 0)$. Let B be the boundary singular point of coordinates $L/4(3, \sqrt{3})$ and C its symmetric

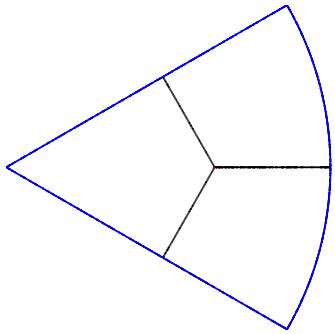

FIGURE 14. Symmetric candidate for $\Sigma_{\pi/3}$.

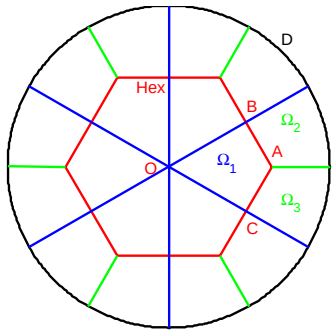

FIGURE 15. Tiling of the disk with the 3-partition of Figure 14.

point with respect to the axis $\{y = 0\}$. The area of the total disk $Disk$ equals $\mathcal{A}(Disk) = \pi$. The area of the regular hexagon plotted in red in Figure 15 is

$$\mathcal{A}(\text{Hex}) = \frac{3\sqrt{3}}{2}L^2.$$

We deduce

$$\mathcal{A}(\Omega_1) = \frac{\sqrt{3}L^2}{4}.$$

Let us now compute the area of Ω_2. We have

$$\mathcal{A}(\Omega_2) = \frac{1}{12}(\mathcal{A}(Disk) - \mathcal{A}(\text{Hex})) = \frac{2\pi - 3\sqrt{3}L^2}{24}.$$

With $L = 0.64$, we obtain

$$\mathcal{A}(\Omega_1) \simeq 0.177 \qquad \text{and} \qquad \mathcal{A}(\Omega_2) \simeq 0.173.$$

Since the accuracy on L is 10^{-2}, this gap is not significant. Let us determine now for which value of L we have the equality:

$$\mathcal{A}(\Omega_1) = \mathcal{A}(\Omega_2) \iff \frac{\sqrt{3}L^2}{4} = \frac{2\pi - 3\sqrt{3}L^2}{24} \iff L = \sqrt{\frac{2\pi}{9\sqrt{3}}} \simeq 0.634\ 875.$$

In this case, we have $\mathcal{A}(\text{Hex}) = \pi/3$.

This result is coherent with the discretization step for x_α which equals $1/100$. Therefore it seems that the areas of every domains of the partition are equal.

6. **Laplacian on the double covering.** The method proposed in Section 5 can only catch symmetric candidates. However, we have seen in Figure 7 that for the angle $\alpha = \alpha_3^1$, there exists non symmetric minimal 3-partitions. So we would like to find a method to catch non symmetric candidates. The method we use now was introduced in [4] to explain why we find two symmetric configurations with the same energy in the square. Let us explain this method. Let us go back to a general bounded open and simply connected set Ω with piecewise $\mathcal{C}^{1,+}$ boundary. In the non nodal case, there are three topological types possible for a minimal 3-partition of such a domain. They are given by configuration (a), (b), and (c) in Section 5, removing the symmetry assumption. As suggested by the numerical study of the symmetric case, we only look for minimal partitions of type (a). Then, there is an interior singular point where three half-curves meet. Following [4], we consider a double Riemannian covering of the domain Ω punctured by this point. We then look for a minimal partition of Ω as the projection of a nodal partition of the double covering.

6.1. **Double covering of the domain.** We will give a rather informal description of the double covering. Let us consider a point $X_0 \in \Omega$. We denote $\Omega \setminus \{X_0\}$ by Ω_{X_0}. We now choose a simple regular curve γ contained in Ω that links X_0 to a point in $\partial\Omega$. We consider two copies of $\Omega \setminus \gamma$ that we glue in such a way that a side of γ on one sheet is connected to the opposite side on the other sheet (cf. Figure 16). The resulting object is a two dimensional manifold with boundary, that we denote by $\widetilde{\Omega}_{X_0}$, with a natural projection map $\Pi : \widetilde{\Omega}_{X_0} \to \Omega_{X_0}$. It is a double covering of Ω_{X_0}, that we equip with the Riemannian metric lifted from Ω_{X_0} through Π. A rigorous and general construction is explained in [13]. In particular, it can be shown that the result does not depend on the choice of γ.

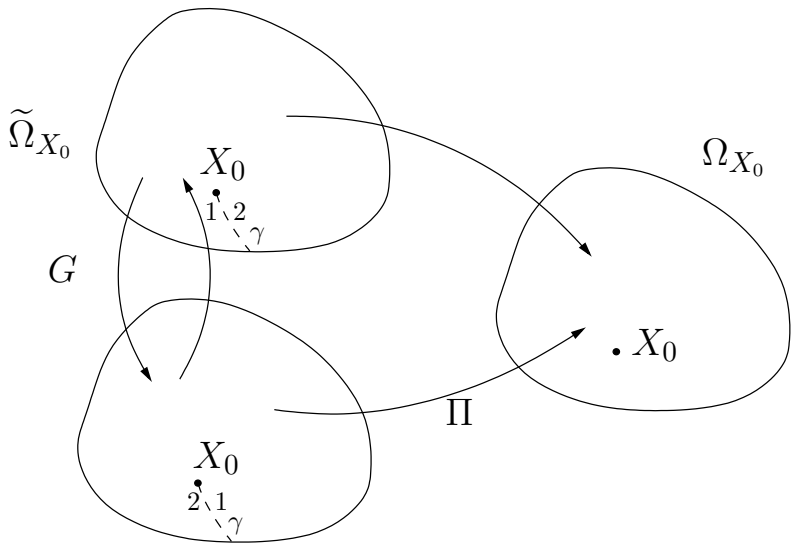

FIGURE 16. Double covering of Ω_{X_0}.

6.2. **Symmetric and antisymmetric eigenvalues.** Let us now define a mapping G from $\widetilde{\Omega}_{X_0}$ onto itself, called the *deck map*. For any $X_1 \in \widetilde{\Omega}_{X_0}$, $G(X_1)$ is the only element $X_2 \in \widetilde{\Omega}_{X_0}$ such that $X_2 \neq X_1$ and $\Pi(X_2) = \Pi(X_1)$. Intuitively, the mapping G moves points from one sheet of the double covering to the other one. We have of course $G^2 = \mathrm{Id}$. A function $f : \widetilde{\Omega}_{X_0} \to \mathbb{C}$ is said to be *symmetric* if $f \circ G = f$ and *antisymmetric* if $f \circ G = -f$. If we call $\mathcal{S}$ (resp. $\mathcal{A}$) the space of functions in $L^2(\widetilde{\Omega}_{X_0})$ that are symmetric (resp. antisymmetric), we have the orthogonal decomposition:

$$L^2(\widetilde{\Omega}_{X_0}) = \mathcal{S} \oplus \mathcal{A}.$$

We call *lifted Laplacian* the Laplace-Beltrami operator on $\widetilde{\Omega}_{X_0}$ with Dirichlet boundary condition. The lifted Laplacian preserves symmetric and antisymmetric functions. We can therefore choose a basis of eigenfunctions for each subspace $\mathcal{S}$ and $\mathcal{A}$. Their reunion is a basis of eigenfunctions for $L^2(\widetilde{\Omega}_{X_0})$. The eigenvalues associated with a symmetric (resp. antisymmetric) eigenfunction will be called *symmetric* (resp. *antisymmetric*). The symmetric eigenvalues are actually the eigenvalues of the Dirichlet Laplacian on Ω, since any symmetric eigenfunction is lifted from an eigenfunction on Ω_{X_0}. We call the antisymmetric eigenvalues *Aharonov-Bohm* eigenvalues, denoted by λ_k^{AB}, since they can be considered as the eigenvalues of a so-called *Aharonov-Bohm* operator with pole at $X = X_0$ and flux $\Phi = 1/2$ (cf. [1, 13, 2, 21]).

Let us now consider a nodal partition $\mathcal{D} = \{D_i : 1 \leq i \leq \ell\}$ associated with an antisymmetric eigenfuction u. The image of a domain of $\mathcal{D}$ by the deck map G is another domain where u has the opposite sign. We can therefore group together the domains of $\mathcal{D}$ in pairs $\{D_i, D_j\}$ such that $D_i \cap D_j = \emptyset$ and $\Pi(D_i) = \Pi(D_j)$. The set $\Pi(\mathcal{D}) = \{\Pi(D_i) : 1 \leq i \leq \ell\}$ is then a strong k-partition of Ω, with $2k = \ell$ (we deduce in particular that ℓ is even). Furthermore, contrary to $\mathcal{D}$, the partition $\Pi(\mathcal{D})$ is not necessarily bipartite. We will use this to build non nodal candidates to be a minimal k-partition.

Consequently, if we find for some α a singular point X such that there exists an antisymmetric eigenfunction with 6 nodal domains and associated with $\lambda_6(\widetilde{(\Sigma_\alpha)_X})$ such that

$$\lambda_6(\widetilde{(\Sigma_\alpha)_X}) < \Lambda_3(\mathcal{D}_\alpha^{sym}),$$

then the symmetric 3-partition $\mathcal{D}_\alpha^{sym}$ is not minimal. Indeed, the projection of this sixth eigenfunction on the first sheet is a 3-partition whose energy is less than $\Lambda_3(\mathcal{D}_\alpha^{sym})$.

We have another way of checking that a 3-partition is not minimal. According to [16, Remark 5.2], a minimal 3-partition must be Courant-sharp for the Aharonov-Bohm operator, that is to say, its energy must be λ_3^{AB}.

Let us now combine the double covering approach and the results of Section 5 to obtain more information. The first result consists in invalidating possibly some candidates of type (a1) obtained in Subsection 5.1. Let us use the best candidates obtained in Subsection 5.1. For any $\alpha \in \{k\pi/100, 16 \leq k \leq 76\}$, we compute the first eigenvalues of the Dirichlet Laplacian on the double covering $\widetilde{(\Sigma_\alpha)_X}$ with $X = (\tilde{x}_\alpha^{ND}, 0)$ and we split the spectrum between the symmetric eigenvalues $\lambda_k(\Sigma_\alpha)$ and the antisymmetric ones $\lambda_k^{AB}((\Sigma_\alpha)_X)$. Figure 17 gives the first seven eigenvalues on $\widetilde{(\Sigma_\alpha)_X}$ and the nodal partition of the eigenfunctions are represented on Figure

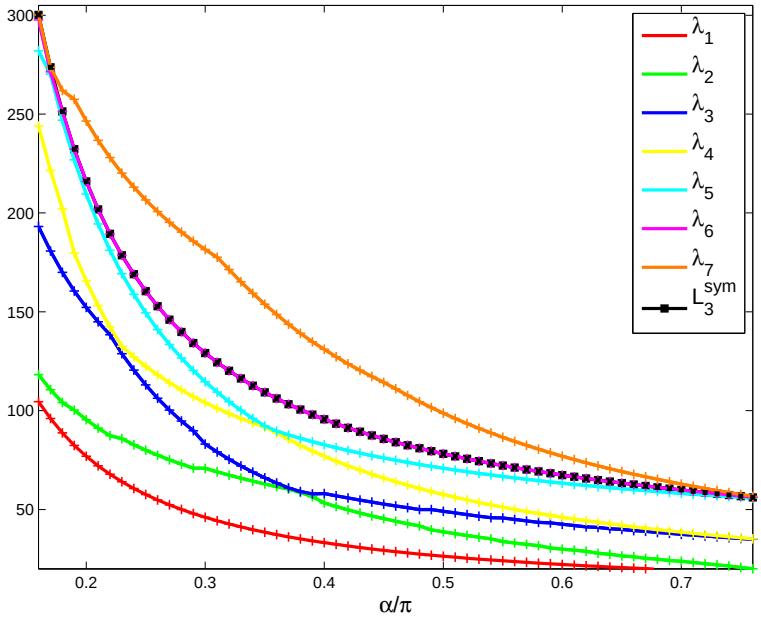

FIGURE 17. $\lambda_j((\widetilde{\Sigma_\alpha})_X)$, with $X = (\tilde{x}_\alpha^{ND}, 0)$, $\alpha \in \{\frac{k\pi}{100}, 16 \leq k \leq 76,\ 1 \leq j \leq 7\}$.

18 for several α. We notice that

$$\Lambda_3(\mathcal{D}_\alpha^{sym}) = \lambda_7((\widetilde{\Sigma_\alpha})_X) = \lambda_4^{AB}((\Sigma_\alpha)_X) > \lambda_5((\widetilde{\Sigma_\alpha})_X) = \lambda_3^{AB}((\Sigma_\alpha)_X), \text{ for } \alpha = \frac{16\pi}{100},$$

$$\Lambda_3(\mathcal{D}_\alpha^{sym}) = \lambda_7((\widetilde{\Sigma_\alpha})_X) = \lambda_4^{AB}((\Sigma_\alpha)_X) > \lambda_6((\widetilde{\Sigma_\alpha})_X) = \lambda_3^{AB}((\Sigma_\alpha)_X), \text{ for } \alpha = \frac{17\pi}{100},$$

$$\Lambda_3(\mathcal{D}_\alpha^{sym}) = \lambda_6((\widetilde{\Sigma_\alpha})_X) = \lambda_3^{AB}((\Sigma_\alpha)_X), \text{ for } \alpha \in \{\frac{k\pi}{100},\ k = 18, \ldots, 76\}.$$

Consequently, the minimal symmetric 3-partition $\mathcal{D}_\alpha^{sym}$ is not minimal for $\alpha = 16\pi/100$ and $\alpha = 17\pi/100$.

To make simulations, we use the techniques we have previously explained in [3]: this consists in meshing the double covering for the domain and using the Finite Element Library MÉLINA (see [19]).

6.3. **Numerical simulations for non symmetric candidates.** Let us consider an angle $\alpha = \alpha_3^1 + \varepsilon$ with ε very small and positive. We have seen that the 3-partition $\mathcal{D}_\alpha^{sym}$ is not minimal when ε is small enough.

We would like to use the double covering approach to catch some non symmetric candidates. For any point $X \in \Omega$, we compute the first six eigenvalues of the Dirichlet Laplacian on the double covering $(\widetilde{\Sigma_\alpha})_X$. The symmetric eigenvectors are those of the Dirichlet Laplacian on Σ_α and we are interested in the antisymmetric ones. We move the puncturing point on Σ_α and hope to find a 3-partition given by the 6-th eigenfunction of the Dirichlet Laplacian on $(\widetilde{\Sigma_\alpha})_X$.

Proposition 6 gives us an idea to localize the puncturing point X. Starting with Σ_α for $\alpha = \alpha_3^1$, we can pick an eigenfunction whose nodal set has a boundary singular point with polar coordinates $(\rho_c, \alpha_3^1/2)$. Its nodal partition has three domains and

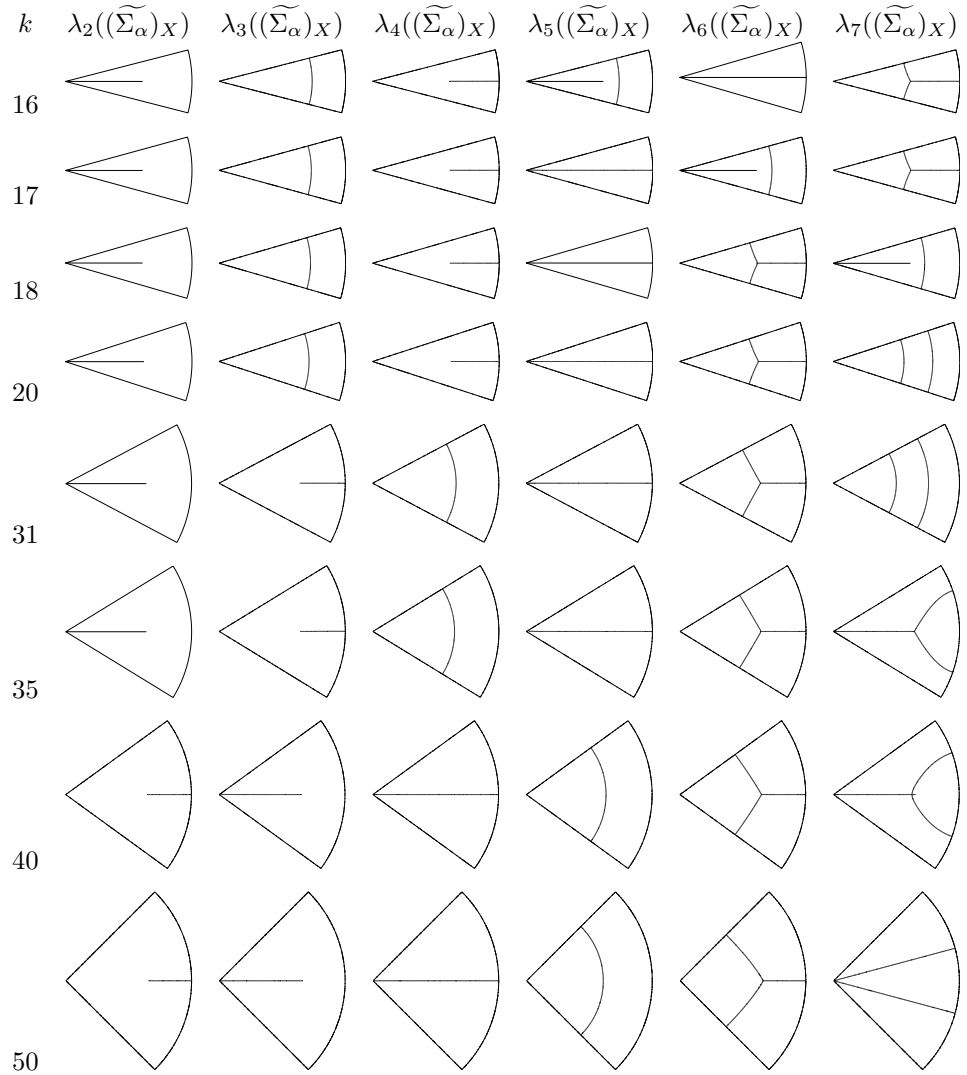

FIGURE 18. Nodal partition associated with $\lambda_j((\widetilde{\Sigma_\alpha})_X)$, $X = (\tilde{x}_\alpha^{ND}, 0)$, $\alpha = \frac{k\pi}{100}$, $2 \leq j \leq 7$.

a boundary singular point at $(\rho_c, \alpha_3^1/2)$ where two lines meet. We recall that at a singular point, nodal lines satisfy the equal angle property. We can use this property to localize a possible singular point for Σ_α with $\alpha = \alpha_3^1 + \varepsilon$. If the minimal 3-partition for Σ_α has a singular point on the boundary $\{y = x \tan\frac{\alpha}{2}\}$ with only one nodal line reaching this point, then this nodal line is normal to the boundary at the singular point. If ε is very small, the distance between this singular point and the origin should be close to ρ_c.

When the angle is increasing, this approximation is not efficient. For $\alpha = \pi/3$, the boundary singular point seems to have polar coordinates $(\rho_3, \pi/6)$ with $\rho_3 = L\sqrt{3}/2 \simeq 0.5498$.

For numerical computations, we choose X on some perpendicular axes to the boundary (see Figure 19):

$$X \in \{X_k = (1 - \tfrac{k}{100})C_\rho + \tfrac{k}{100}A_\rho, 0 \le k \le 100\},$$

where C_ρ and A_ρ are the points of coordinates

$$C_\rho = \rho(\cos\tfrac{\alpha}{2}, \sin\tfrac{\alpha}{2}) \text{ and } A_\rho = \rho(1/\cos\tfrac{\alpha}{2}, 0), \quad \text{with } \rho \in \{0.54 + k/50, k = 0, \dots, 6\}.$$

Then we catch a 3-partition among the 6-th eigenfunction of the Dirichlet Laplacian on $\widetilde{(\Sigma_\alpha)}_X$. With this method, we obtain, for several values of α, new partitions $\mathcal{D}_\alpha^{AB}$ better than the minimal symmetric 3-partition $\mathcal{D}_\alpha^{sym}$ obtained by the mixed Neumann-Dirichlet approach (see Figure 20).

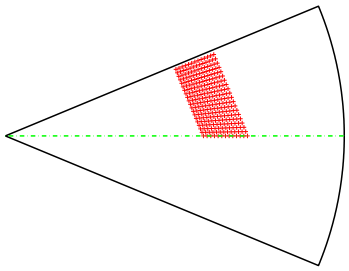

FIGURE 19. Localization of the puncturing point for numerical simulations, $\alpha = 0.5$.

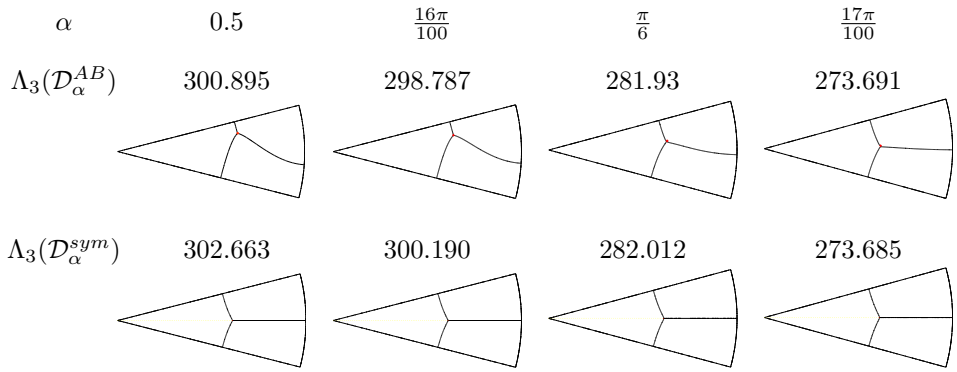

FIGURE 20. Candidates for the minimal 3-partition of Σ_α.

For different sectors, we proceed in the same way and obtain new candidates whose energy is represented in orange color in Figure 12 (see also Figure 20). We obtain a better candidate than the symmetric one for angles close to α_3^1 and especially for $\alpha = 16\pi/100$ and $\alpha = \pi/6$. For larger angles, the double covering approach gives candidates whose energy is so close to those of the symmetric candidates that we cannot be affirmative. This is probably due to the fact that the best candidate obtained by the double covering approach has an interior singular point close to (or on) the symmetry axis for larger α and then, by continuity, the eigenvalues are close to those of the mixed Neumann-Dirichlet Laplacian.

Notice that for $\alpha = \alpha_3^2$, all candidates in Figure 8 are symmetric. This encourages us to make the conjecture:

Conjecture 1. *There exists α_3^3 such that*

- *for $\alpha \in (\alpha_3^1, \alpha_3^3)$, the minimal 3-partitions are non symmetric,*
- *for $\alpha \in (\alpha_3^3, \alpha_3^2)$, any minimal 3-partition is symmetric.*

7. Negative results for minimal k-partitions, $k = 4, 5, 6$.

7.1. 4-partition.

Figure 21 represents the eigenvalues $\lambda_{m,n}(\alpha)$ for $(m,n) = (1,4)$, $(2,2)$, $(4,1)$ and $\lambda_4(\alpha)$ given by (2) computed with the MATLAB software and illustrates the lower and upper bounds for $\mathfrak{L}_4(\Sigma_\alpha)$:

$$\lambda_4(\alpha) \leq \mathfrak{L}_4(\Sigma_\alpha) \leq \min(\lambda_{1,4}(\alpha), \lambda_{2,2}(\alpha), \lambda_{4,1}(\alpha)).$$

Since $\lambda_{2,2}(\alpha) > \lambda_4(\alpha)$, partitions having the topology of $u_{2,2}$ and illustrated in Figure 22 cannot be minimal for any α.

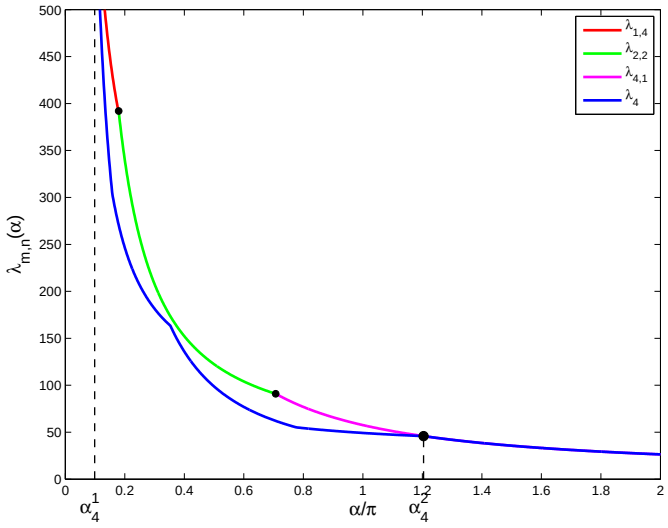

FIGURE 21. Lower and upper bounds for $\mathfrak{L}_4(\Sigma_\alpha)$.

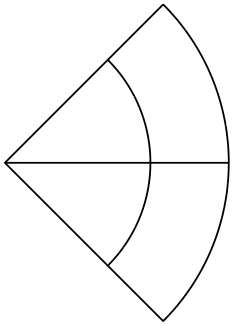

FIGURE 22. Non minimal 4-partition.

7.2. **5-partition.** Since $k = 5$ is a prime number, we only have the bounds given by Proposition 5 and Remark 3:

$$\mathfrak{L}_5(\alpha) = \lambda_5(\alpha) \qquad \text{for } \alpha \in (0, \alpha_5^1] \cup [\alpha_5^2, 2\pi],$$
$$\lambda_5(\alpha) < \mathfrak{L}_5(\alpha) < L_5(\Sigma_\alpha) \leq \min(\lambda_{1,5}(\alpha), \lambda_{5,1}(\alpha)) \qquad \text{for } \alpha \in (\alpha_5^1, \alpha_5^2).$$

Figure 23 illustrates these estimates using the MATLAB software.

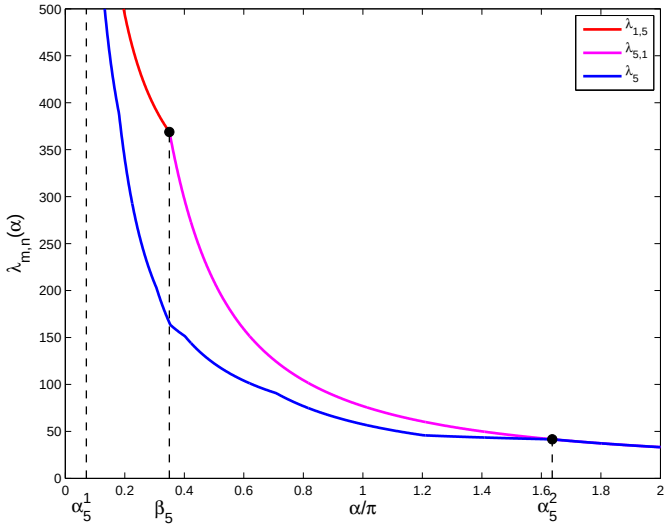

FIGURE 23. Lower and upper bounds for $\mathfrak{L}_5(\Sigma_\alpha)$.

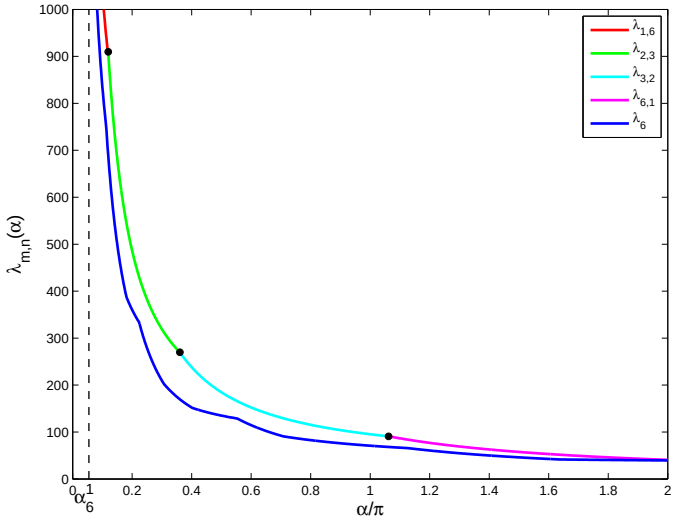

FIGURE 24. Lower and upper bounds for $\mathfrak{L}_6(\Sigma_\alpha)$.

7.3. **6-partition.** Using Figure 24 (obtained by the MATLAB software), we notice that

$$\min(\lambda_{2,3}(\alpha), \lambda_{3,2}(\alpha), \lambda_{6,1}(\alpha)) > \lambda_6(\alpha), \qquad \forall \alpha \in (0, 2\pi].$$

Thus candidates of the types illustrated in Figure 25 (i.e. having the topologies of the eigenfunctions $u_{2,3}$, $u_{3,2}$ and $u_{6,1}$) are never minimal.

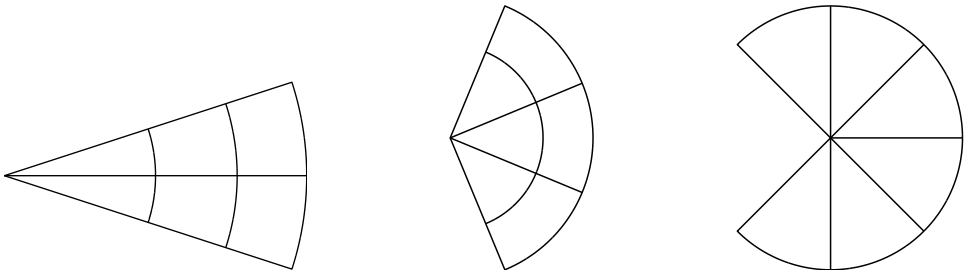

FIGURE 25. Non minimal 6-partitions.

Acknowledgments. The authors thank Bernard Helffer for many suggestions and discussions concerning this work. This work was partially supported by the ANR (Agence Nationale de la Recherche), projects GAOS n° ANR-09-BLAN-0037-03 and OPTIFORM n° ANR-12-BS01-0007-02. The first author is grateful to the Mittag-Leffler Institute where this paper was achieved.

REFERENCES

[1] Y. Aharonov and D. Bohm, Significance of electromagnetic potentials in the quantum theory, *Phys. Rev.*, **115** 1959, 485–491.
[2] B. Alziary, J. Fleckinger-Pellé and P. Takáč, Eigenfunctions and Hardy inequalities for a magnetic Schrödinger operator in $\mathbb{R}^2$, *Math. Methods Appl. Sci.*, **26** (2003), 1093–1136.
[3] V. Bonnaillie-Noël and B. Helffer, Numerical analysis of nodal sets for eigenvalues of Aharonov-Bohm Hamiltonians on the square with application to minimal partitions, *Exp. Math.*, **20** (2011), 304–322.
[4] V. Bonnaillie-Noël, B. Helffer and T. Hoffmann-Ostenhof, Aharonov-Bohm Hamiltonians, isospectrality and minimal partitions, *J. Phys. A*, **42** (2009), 185203, 20.
[5] V. Bonnaillie-Noël, B. Helffer and G. Vial, Numerical simulations for nodal domains and spectral minimal partitions, *ESAIM Control Optim. Calc. Var.*, **16** (2010), 221–246.
[6] D. Bucur, G. Buttazzo and A. Henrot, Existence results for some optimal partition problems, *Adv. Math. Sci. Appl.*, **8** (1998), 571–579.
[7] M. Conti, S. Terracini and G. Verzini, An optimal partition problem related to nonlinear eigenvalues, *J. Funct. Anal.*, **198** (2003), 160–196.
[8] M. Conti, S. Terracini and G. Verzini, On a class of optimal partition problems related to the Fučík spectrum and to the monotonicity formulae, *Calc. Var. Partial Differential Equations*, **22** (2005), 45–72.
[9] M. Conti, S. Terracini and G. Verzini, A variational problem for the spatial segregation of reaction-diffusion systems, *Indiana Univ. Math. J.*, **54** (2005), 779–815.
[10] R. Courant and D. Hilbert, *Methods of mathematical physics. Vol. I*, Interscience Publishers, Inc., New York, N.Y. 1953.
[11] E. C. M. Crooks, E. N. Dancer and D. Hilhorst, On long-time dynamics for competition-diffusion systems with inhomogeneous Dirichlet boundary conditions, *Topol. Methods Nonlinear Anal.*, **30** (2007), 1–36.
[12] *NIST Digital Library of Mathematical Functions*, Online companion to [20], Release 1.0.5 of 2012-10-01. Available from: http://dlmf.nist.gov/.

[13] B. Helffer, M. Hoffmann-Ostenhof, T. Hoffmann-Ostenhof and M. P. Owen, Nodal sets for groundstates of Schrödinger operators with zero magnetic field in non-simply connected domains, *Comm. Math. Phys.*, **202** (1999), 629–649.
[14] B. Helffer and T. Hoffmann-Ostenhof, *On minimal partitions: New properties and applications to the disk*, in *Spectrum and Dynamics*, 52 of CRM Proc. Lecture Notes, 119–135. Amer. Math. Soc., Providence, RI 2010.
[15] B. Helffer and T. Hoffmann-Ostenhof, *Minimal partitions for anisotropic tori*, *J. Spectr. Theory*, (À paraître) (2013).
[16] B. Helffer and T. Hoffmann-Ostenhof, On a magnetic characterization of spectral minimal partitions, *Journal of the European Mathematical Society*, (À paraître) (2013).
[17] B. Helffer, T. Hoffmann-Ostenhof and S. Terracini, Nodal domains and spectral minimal partitions, *Ann. Inst. H. Poincaré Anal. Non Linéaire*, **26** (2009), 101–138.
[18] B. Helffer, T. Hoffmann-Ostenhof and S. Terracini, On spectral minimal partitions: the case of the sphere, in *Around the Research of Vladimir Maz'ya. III*, 13 of Int. Math. Ser. (N. Y.), 153–178. Springer, New York 2010.
[19] D. Martin, *Mélina, Bibliothèque de Calculs éléments Finis*, 2007. Available from: `http://anum-maths.univ-rennes1.fr/melina`.
[20] F. W. J. Olver, D. W. Lozier, R. F. Boisvert and C. W. Clark, *NIST Handbook of Mathematical Functions*, Cambridge University Press, New York, NY 2010. Print Companion to [12].
[21] K. Pankrashkin and S. Richard, Spectral and scattering theory for the Aharonov-Bohm operators, *Rev. Math. Phys.*, **23** (2011), 53–81.

Received December 2012; revised July 2013.

E-mail address: `bonnaillie@math.cnrs.fr`
E-mail address: `corentin.lena@math.u-psud.fr`